CHEMICAL ENGINEERING TRANSACTIONS
VOL. 59, 2017
A publication of AIDIC
The Italian Association of Chemical Engineering
Online at www.aidic.it/cet
Guest Editors: Zhuo Yang, Junjie Ba, Jing Pan

ISBN 978-88-95608- 49-5; **ISSN** 2283-9216
DOI: 10.3303/CET1759110

Research on Optical Fiber Gas Sensing Based on Absorption Spectrometry in Optical Communication

Na Zhang

Xichang College, Xichang 615000, China
zhangna2112@163.com

The Internet of things (IOT) is one of the most popular research fields at present, and the optical fiber sensing network is an important part of the Internet of things. In the field of environmental protection and modern industrial production, there is a need for a sensor network which can monitor the gas concentration information. Because of the strong anti-interference ability, intrinsic safety, optical communication technology-based, intelligent monitoring and other significant characteristics, optical fiber gas sensing equipment and scheme has become the main direction of the field of domestic and foreign research. In this paper, we presents a 1665nm methane sensor structure based on single fiber coupler ring, and the performance of the sensor is analyzed, including the relationship between the optimal ratio of 1550nm coupler in the 1665nm system and the number of rings of signal light. Compared with the traditional absorption spectrum method, the effective absorption length of the chamber is increased 4 times by the sensor. Methane gas samples of two groups were measured by the sensor, and the measurement error was less than 2.5%.

1. Introduction

With the rapidly development of global industrialization and the rapidly increase of global population, the global environment is becoming worse and worse. Air pollution, greenhouse effect and other environmental problems have become the focus of attention because of the serious threat to human health, the earth's ecological environment, biodiversity and climate. In order to solve the problem of air pollution, it is the key to control and monitor the emission of gaseous pollutants (Arapatsakos et al., 2015; Cuisinier et al, 2013; Cannistraro et al., 2015). In addition, in the industrial production, it should timely and accurately monitor, forecast, alarm and take corresponding measures to the flammable, toxic and harmful gas to ensure the order of life, to ensure the safety of people's lives and property of the enterprise, which has become an important problem of petroleum chemical industry, electric power, electrical and other industries (Castellanos-Gomez et al, 2016). In the actual application of sensor, the understanding to the gas concentration of individual monitoring points is not enough, in order to accurately forecast, it must master the gas concentration distribution in a large range and forecast its trend over time, in order to take corresponding measures before the disaster (Wild et al, 2014). So, no matter in the field of environmental protection or modern industrial production, the safe, reliable and stable system that can monitor the gas concentration in many points is needed. The Internet of things, wireless sensor networks and optical fiber sensing network have become the focus and the main direction of the field of domestic and foreign research.

2. Theory and method

2.1 Cavity ring-down spectroscopy

Cavity ring-down spectroscopy (Long, et al, 2014) is an absorption spectroscopy appeared in 80s in last century. The technology has an effective path length and high sensitivity, and is not affected by the instability of light source, so it has attracted attention. A typical cavity ring-down spectroscopy system is shown in Figure 1 (Truong et al, 2013). The system consists of a laser source, a high reflectivity mirror composed of a resonator and an oscilloscope. The light emitted by the laser enters into the cavity, and is restricted to travel between the two high reflectivity mirror oscillation (Renganathan et al, 2014). Each oscillation will carry sense

Please cite this article as: Na Zhang, 2017, Research on optical fiber gas sensing based on absorption spectrometry in optical communication, Chemical Engineering Transactions, 59, 655-660 DOI:10.3303/CET1759110

information because of the loss by the substances to be measured, and a small part of light will be transmitted into the oscilloscope every oscillation.

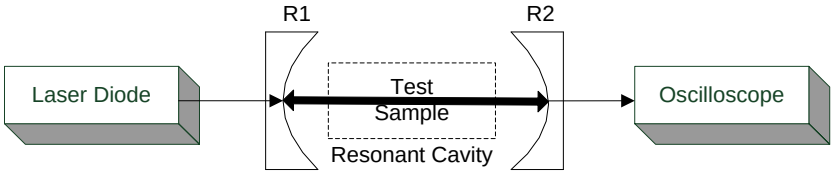

Figure 1: A Principle architecture of Cavity Ring-Down Spectroscopy System

The R1 and R2 in the figure are high reflectivity mirrors. The relationship between the intensity of transmitted light and time can be expressed by (1).

$$I_t(t,\lambda) = I_0(\lambda)\exp\left(-\frac{t}{\tau_e(\lambda)}\right) \tag{1}$$

$I_0(\lambda)$ is the initial intensity of the optical signal with λ wavelength in the cavity. $I_t(t, \lambda)$ is the initial intensity of the optical signal with λ wavelength in the t moments. The ring-down time of optical signal with λ wavelength is defined as the time required in the attenuation of the transmission light intensity to the initial intensity. It is related to all the loss in the cavity, including the measured medium absorption loss and other losses (medium scattering loss, mirror transmission, diffraction and scattering loss etc.). *RDT* $\tau_e(\lambda)$ can be obtained from (1).

$$\tau_e(\lambda) = \frac{nL}{cA} \tag{2}$$

n is the refractive index of the cavity, L is the cavity length of the resonant cavity, C is the velocity of light in vacuum, and the total loss of the cavity is A, $\tau_e(\lambda)$ is the time of the λ optical signal, which is related to the loss of the cavity. According to (3), the down time is only related to the physical parameters of the resonator, and it is not affected by the incident light intensity $I_0(\lambda)$. When the sample in the cavity introduces the loss such as absorption, the total loss of A increases which can make the ring down time become small. The loss of the cavity can be obtained by measuring the attenuation variation down time after inducing the additional loss, and then the additional value of the loss can be obtained. The principle of measurement can be described as follows:
When the sample is not present in the cavity, the formula (2) can be written as:

$$\tau_0 = \frac{nL}{c(1-R)} \tag{3}$$

When the concentration C was measured in the ring cavity, the refractive index of the sample was ignored when the absorption coefficient α of the λoptical signal was measured. At this point, (3) can be written as:

$$\tau_{sample} = \frac{nL}{c[\alpha CL + (1-R)]} \tag{4}$$

Therefore, the concentration C of the medium to be measured can be obtained.

$$C = \frac{n}{\alpha_{absorption} c}\left(\frac{1}{\tau_{sample}} - \frac{1}{\tau_0}\right) \tag{5}$$

It can be seen that the concentration C of the sample to be measured is only related to the transmission rate *c/n* of light in the cavity and the absorption coefficient of the sample. From (3) and (5) we can see that τ_{sample} and τ_0 are related to the transmission speed *c/n* of light, the cavity length L and the reflectivity of the endoscopic. The medium of n with high refractive index is filled with the resonant cavity, or the cavity length and the the reflectivity of the endoscopic are increased, so the corresponding splitting ratio of the coupling in FLCRD is reduced or the loss in ring is decreased, which can increase the ringdown time, so as to improve the measurement accuracy.

2.2 Fiber ring methane gas sensor

Gas absorption chamber (Renganathan, et al, 2017) is one of the key components in the absorption spectrum gas sensor. In order to improve the sensitivity of detection, it often needs a long absorption chamber. The gas chamber in the laboratory has a longer effective length, which needs to reach about 50cm. Based on the absorption spectrum of the sensor, the signal light source must be aligned with the methane absorption peak. In the past, most of the methane sensors use 1310nm wavelength light source, and the absorption coefficient is small. In this paper, a 1650nm wavelength light source is developed, which uses the Super-luminescent Light Emitting Diode with 1653nm center wavelength and 54nm Full Maxmium Half Width (Mishra et al, 2015) as the light source, measuring the peak position and depth of the methane gas in the range of 1600-1700nm by using the AQ6317C spectrometer of ANDO company. At the same time, in order to realize the measurement of the ring down cavity, the light source must be a pulse laser which can generate the pulse, and the width and the repetition period can be adjusted.
Figure 2 shows the connection of the Distributed Feed-Back Laser Diode which the working wavelength is 1665nm laser and oscillograph LeCory WavePro 7000 to the 2 and 4 port of the coupling device, respectively. (DFB LD: Distributed Feed-Back Laser distributed feedback Diode LeCory WavePro 7000), the oscilloscope (OSC: oscillograph) respectively and the coupling device 2 and 4 port connection. The utility model is characterized in that a pair of collimators with a working distance of 50mm is fixed in the V groove to be loaded into the air chamber. The two ends of the collimator are respectively connected with the 1 and the 3 ports of the coupling device to form a closed fiber ring.

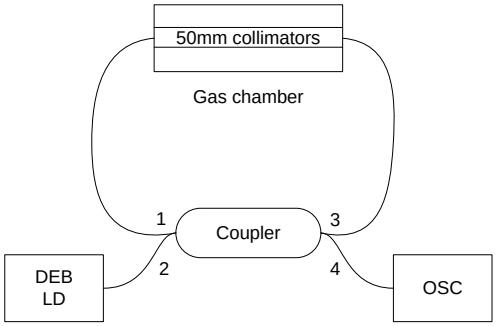

Figure 2: The experimental setup of the fiber loop gas sensor

OFB LD can give out a pulse of light into the fiber ring every certain period, and the output pulse sequence is shown by the receiver. The down time $RDT\,\tau_e$ of the output signal light is related to the loss in the ring, which can be expressed as:

$$\frac{\tau_e}{T} = \frac{10\lg e}{\alpha} \tag{6}$$

T is the time that the signal light travels a round in the ring. The length of the fiber is 20 meters in the experiment, then the corresponding single ring time T is 100ns. A is the total loss of optical signals of a round, then α=fibre loss + collimator loss + coupler loss + absorption loss, and the unit of the loss is dB.
In order to make the relationship between the loss parameter and the concentration more obvious and easier to solve, the relationship between the concentration of the gas to be measured and the fitting coefficient is derived directly from the Beer-Lambert law and after combined with the diffusion coefficient:

$$10\lg\left(\frac{I_i}{I_0}\right) = 10\lg\left(\exp\left[\alpha_\lambda LC\right]\right) \tag{7}$$

The I_i is the size of input light intensity, I_0 is the size of the output light intensity, and the α_λ is the absorption coefficient when the wave length is λ, L is the length of the chamber, C is the gas concentration. So it can be defined that on the left side of the equation is the gas absorption loss of the single circle, and the unit is dB, then we can get:

$$\alpha_g = \alpha_\lambda LC \times 10\lg e \tag{8}$$

The total loss α of the single ring is the sum of the gas absorption loss α_g and the insertion loss α_s of the system:

$$\alpha = 4.34\alpha_\lambda LC + \alpha_s \tag{9}$$

L is 50mm, and α_λ can be obtained after combined with data in HITRAN database, and the relationship between the concentration C and total loss α can be obtained according to the above formula. It can be seen from the experimental results that the diffusion time and the residual gas concentration in the gas diffusion are in accordance with the following exponential decay:

$$C = a\exp[-bt] + c \tag{10}$$

When the boundary condition t=0, the concentration of C is 100%; when the t approaches infinity, the gas has been diffused out of the gas chamber, and the concentration is 0%. The parameter can be determined as a=1, C=0. The relationship between concentration and time can be expressed as:

$$C = \exp[-bt] \tag{11}$$

The relationship between the diffusion time and total loss can be obtained according (10):

$$\alpha = 4.34\alpha_\lambda L\exp[-bt] + \alpha_s \tag{12}$$

In order to simplify the calculation, in this paper, we proposed a single loop attenuation coefficient B. The single loop attenuation coefficient B is defined as the ratio of the single ring time τ_e to the attenuation time:

$$B = T/\tau_e \tag{13}$$

3. Result and analysis

3.1 System calibration

The gas path is the key part of the gas sensor, and an adjustable and controllable gas path is the base of the gas sensing experiment, including the gas source, gas path control and gas path detection. In order to ensure the accuracy of the measurement of the concentration of the gas chamber in the experiment period, the change of the indoor concentration of the gas should be known, so the the gas diffusion experiment is carried out. Experiment shows that the gas concentration is still stable in the order of ms the extreme case, and when the valve is closed, the air leakage is less than 1% in 24 hours. So it is accurate and effective to use the gas chamber to measure the gas concentration.

The experimental system is built according to figure 2. The signal pulse length is 1665.538nm, the pulse width is 50ns, and the cycle is 1us. In order to test the calibration of the system, the pure methane (purity is >99.9%) is charged into the gas chamber and the valve is opened to record the output pulse sequence after 14 time diffusion. The figure 3 is the pulse sequence single exponential fitting diagram at the 8th, 16th and 108th minutes.

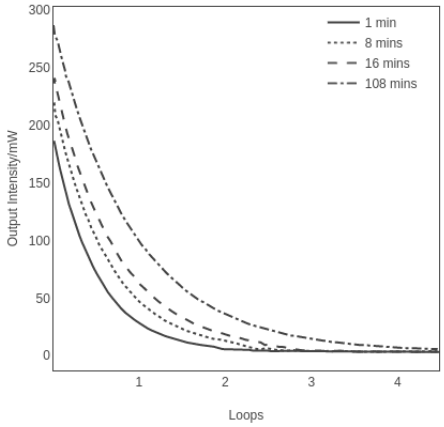

Figure 3: Single exponential fitting curve of output pulse measured at first, 8, 16 and 108 minutes after valve opening

As can be seen in Figure 3, with the change of time, the fitting curve gradually slowed down which reflects the diffusion of gas is slow from the gas chamber to the outside. The fitting coefficients of the 14 records are calculated respectively, and the total loss of each time is obtained and represented by the x in figure 4. After fitting according to (12), it can obtain that p=4631, q=0.07376, r=5.408.

$$\alpha = 4.631e^{(-0.07376t)} + 5.408 \tag{16}$$

When α_s=5.408*db*, the absorption coefficient is α_λ=0.209/*cm,* then the (16) can be:

$$C = (4.34B - 5.408)/4.631 = (\alpha - 5.408)/4.631 \tag{17}$$

After the methane gas is filled into the gas chamber, only the output pulse sequence is recorded by OSC, and the coefficient of B in (17) is obtained according to the single exponential fitting, and the corresponding gas concentration C can be obtained.

3.2 Sample determination

In order to evaluate the error of the scheme, the methane samples A and B of two groups were measured respectively. The concentrations of the samples were 30.7% and 69.8%, respectively. The output pulse sequence is shown in Figure 4. The real curve is the output pulse sequence data recorded by OSC. The × represents the fitting data, and the dashed line represents a single exponential fitting curve.

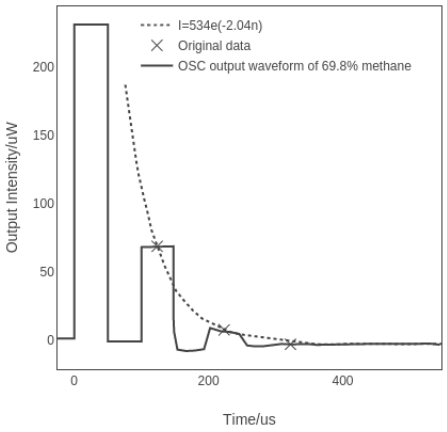

Figure 4: The output waveform and fitting waveform when measuring 69.8% methane gas samples

Table 1: The regression results of the sustainable development of chemical industry ($\hat{C}_2$ is taken as the example)

Sample \ Experiment	1st			2nd			Average	
	B	α /dB	C%	B	α /dB	C%	C_{ave}%	Error/%
A	1.575	6.836	30.8	1.567	6.801	30.1	30.45	0.81
B	1.976	8.576	68.4	2.040	8.854	74.4	71.4	2.29

As can be seen from the table that when the gas concentration is larger, because the fitting series is less that makes the error larger, thus the number of rings is increased by decreasing the loss in the ring, and it is very necessary to increase the ring-down time and series.

4. Conclusions

In 1820s, people began to study the gas detection equipment and methods, there have been a variety types of gas sensors, such as contact combustion type, electrochemical type, semi conductor type, optical fiber type and so on. The optical fiber gas sensing equipment and the scheme have become the focus of attention and research because of its strong anti-interference, intrinsically safe, optical communication technology-based, simple networking, intelligent monitoring and other significant characteristics. In this paper, a single fiber ring 1665nm methane sensor is studied, and the methane 1665nm absorption peak is measured by the sensor. The relationship between the optimal splitting ratio and the number of rings in the sensor is analyzed

theoretically, which is instructive for the selection of the experimental equipment and the improvement of the detection sensitivity. The gas samples of two groups were measured, and the measurement error was less than 2.5% when the effective absorption length of the chamber was increased by a factor of 4 by the sensor.

Reference

Arapatsakos C., Karkanis A., Anastasiadou C., 2015, The load and the gas emissions measurement of outboard engine, International Journal of Heat and Technology, 33(4), 221-228, DOI: 10.18280/ijht.330430

Cuisinier M., Cabelguen P.E., Evers S., He G., Kolbeck M., Garsuch A., Bolin T., Balasubramanian M., Nazar L.F., 2013. Sulfur speciation in Li–S batteries determined by operando X-ray absorption spectroscopy, The Journal of Physical Chemistry Letters, 19(4), 3227-3232.

Cannistraro G., Cannistraro M., Cannistraro A., Galvagno A., Trovato G., 2016, Reducing the demand of energy cooling in the CED, “centers of processing data”, with use of free-cooling systems, International Journal of Heat and Technology, 34(3), 498-502, DOI: 10.18280/ijht.340321.

Castellanos-Gomez A., Quereda J., van der Meulen H.P., Agraït N. and Rubio-Bollinger G., 2016. Spatially resolved optical absorption spectroscopy of single-and few-layer MoS2 by hyperspectral imaging. Nanotechnology, 27(11), 115705.

Wild R.J., Edwards P.M., Dubé W.P., Baumann K., Edgerton E.S., Quinn P.K., Roberts J.M., Rollins A.W., Veres P.R., Warneke C. and Williams E.J., 2014. A Measurement of Total Reactive Nitrogen, NO y, together with NO2, NO, and O3 via Cavity Ring-down Spectroscopy. Environmental science & technology, 48, 16, pp.9609-9615.

Long D.A., Fleisher A.J., Wójtewicz S. and Hodges J.T., 2014. Quantum-noise-limited cavity ring-down spectroscopy. Applied Physics B, 115(2), 149-153.

Truong G.W., Long D.A., Cygan A., Lisak D., van Zee R.D. and Hodges J.T., 2013. Comb-linked, cavity ring-down spectroscopy for measurements of molecular transition frequencies at the kHz-level, The Journal of chemical physics, 138(9), 094201, DOI: 10.1063/1.4792372.

Renganathan B., Sastikumar D., Raj S.G. and Ganesan A.R., 2014. Fiber optic gas sensors with vanadium oxide and tungsten oxide nanoparticle coated claddings, Optics Communications, 315, 74-78.

Mishra S.K., Tripathi S.N., Choudhary V. and Gupta B.D., 2015. Surface Plasmon Resonance-Based Fiber Optic Methane Gas Sensor Utilizing Graphene-Carbon Nanotubes-Poly (Methyl Methacrylate) Hybrid Nanocomposite, Plasmonics, 10(5), 1147-1157.